NANO LETTERS

2007
Vol. 7, No. 4
900−904

Thermal Conductivity Measurements of Semitransparent Single-Walled Carbon Nanotube Films by a Bolometric Technique

Mikhail E. Itkis, Ferenc Borondics,† Aiping Yu, and Robert C. Haddon*

Center for Nanoscale Science and Engineering, Departments of Chemistry and Chemical & Environmental Engineering, University of California, Riverside, California 92521-0403

Received November 16, 2006; Revised Manuscript Received February 25, 2007

ABSTRACT

We introduce a new technique for measurement of the thermal conductivity of ultrathin films of single-walled carbon nanotubes (SWNTs) utilizing IR radiation as heat source and the SWNT film as thermometer. The technique is applied to study the temperature dependence of the thermal conductivity of an as-prepared SWNT film obtained in the electric arc discharge process and a film of purified SWNTs prepared by vacuum filtration. The interplay between thermal and electrical transport in SWNT networks is analyzed in relation to the type of intertube junctions and the possibility of optimizing the thermal and electrical properties of SWNT networks for specific applications is discussed.

Thin films of single-walled carbon nanotubes (SWNTs) attract significant attention because of their outstanding performance in gas and biosensing,[1,2] as a transparent conducting coating for large-area flexible optoelectronics,[3−7] and as the thermal interface layer for heat dissipation in high-density electronic packaging.[8] Recently we suggested the use of semitransparent suspended SWNT films as the sensitive element of infrared bolometric detectors;[9] in contrast to the other applications[1−7] the thermal conductivity of the SWNT film should be minimized in this device in order to achieve high detector sensitivity.

The SWNT film can be envisioned as a network of individual SWNTs and SWNT bundles[7,10,11] in which the thermal and electrical resistances are dominated by the intertube junctions,[7,10−12] which in turn are strongly affected by chemical modification of the SWNTs and the film preparation technology.[11] In order to optimize the preparation of ultrathin SWNT films for specific applications, it would be useful to evaluate their thermal conductivity as a function of preparation technique and functionality. In this Letter we introduce a new bolometric technique to measure the thermal conductivity of suspended semitransparent SWNT films and demonstrate the application of this technique to two very different types of SWNT film preparations.

The thermal conductivity of individual carbon nanotubes (CNTs) has been measured using lithographically defined, microfabricated devices in the case of SWNTs[13] and multiwalled carbon nanotubes (MWNT),[14,15] and by analyzing the Joule heating of suspended SWNTs.[16] The 3ω-technique was also employed for measurement of the thermal conductivity of MWNT ropes[17] and individual MWNTs.[18,19] For macroscopic SWNT samples in the form of fibers or relatively thick SWNT films (buckypaper), of transverse dimensions 1−10 μm, a comparative technique was found to be efficient.[12,20−22] For very thin films (submicrometer range, 10−100 nm), which are required for the SWNT-based IR bolometer[9] and for flexible optoelectronics,[3−7] the heat leakage through the thermocouple wires limits the applicability of the comparative technique.[23] In the present paper we propose a new technique for the measurement of the thermal conductivity of semitransparent SWNT films which are less than 100 nm in thickness and of nanogram mass. In this method the IR radiation is used as a heat source to generate a triangular temperature profile along the suspended SWNT film (Figure 1a), and the SWNT film itself serves as a resistive thermometer, obviating the need for the attachment of external thermometers to the sample.

The SWNT films for this study were prepared using two different techniques. A natural network of as-prepared (AP) SWNTs was self-assembled during the electric arc discharge process,[24] by placement of a stainless steel wire grid around the plasma zone inside the electric arc chamber which nucleates the formation of an extended network (web) from the growing SWNTs as they drift from the plasma core

* Corresponding author. E-mail: haddon@ucr.edu.
† Present address: MTA SzFKI, Budapest, H 1525, Hungary.

10.1021/nl062689x CCC: $37.00
Published on Web 03/27/2007

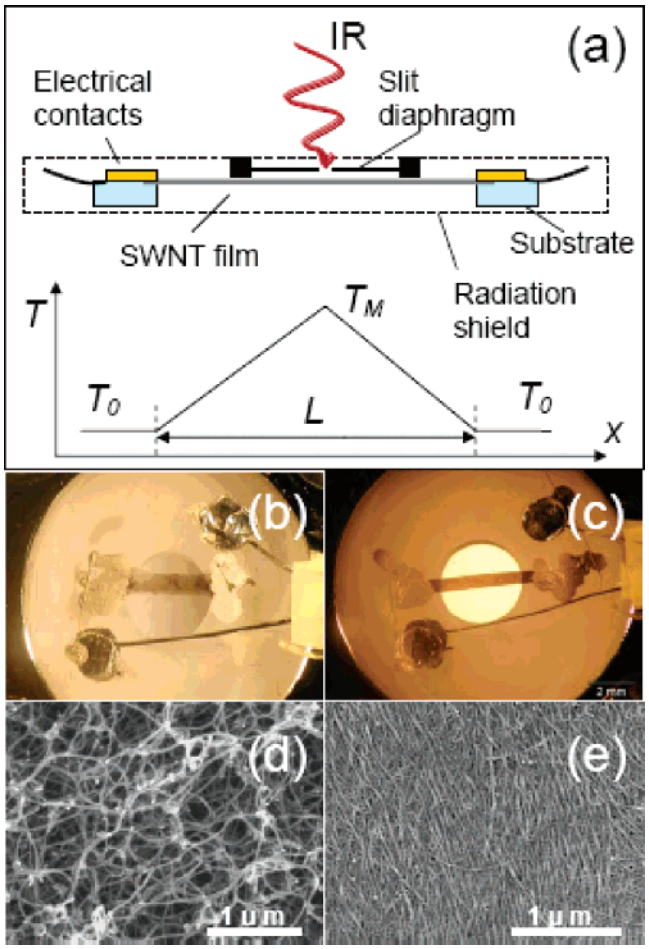

Figure 1. (a) Bolometric configuration for measurement of thermal conductivity of SWNT film suspended between electrical contacts. The heat is provided by IR LED illuminating the SWNT film through the narrow slit diaphragm which generates a triangular temperature profile. (b) Semitransparent film of as-prepared SWNTs film grown in the electric arc discharge chamber and suspended across the opening in a sapphire ring. (c) Semitransparent film of purified SWNTs prepared by vacuum filtration mounted for thermal conductivity measurements. SEM images of fragments of (d) AP-SWNT film, and (e) P-SWNT film. Note that the P-SWNT film is much more densely packed than the AP-SWNT network.

toward the water-cooled walls of the arc reactor and results in a continuous semitransparent SWNT film after 1−5 min of operation.[9,24] In the second preparation technique purified (P) SWNTs were utilized[25] and a free-standing P-SWNT film was obtained by vacuum filtration of a SWNT dispersion according to literature procedures.[3] Due to the mode of preparation, the AP-SWNT film forms a less tightly packed network (Figure 1b,d) than the highly condensed morphology of the P-SWNTs (Figure 1c,e).

The P-SWNT film utilized for thermal conductivity measurements was of thickness $t = 100 \pm 20$ nm (Figure 1c). We calibrated the thickness by first preparing a thick P-SWNT film ($t \sim 5\ \mu$m) using a known weight of P-SWNT material dispersed for the filtration; the weight calculations made use of the area of the filtration membrane and the theoretical packing density of SWNTs (1.4 ± 0.1 g/cm^3).[26] The thickness of the film was measured directly by optical and scanning electron microscopy (SEM), and by a micrometer to give a value of $t = 5.2 \pm 0.7\ \mu$m. By using a microbalance we found a density of 1.5 ± 0.2 g/cm^3 for the SWNT film in close agreement with a theoretical value.[26] On the basis of this calibration we prepared a 100 nm P-SWNT film by utilizing 50 times less material; the resulting thickness of $t = 100 \pm 20$ nm was confirmed by use of near-infrared (NIR) absorption spectroscopy.[11,27,28]

The effective thickness of the AP-SWNT film ($t = 35 \pm 10$ nm) (Figure 1b) was determined by comparing its optical absorption with that of the 100 nm thick P-SWNT film (Figure 1c). The AP-SWNT film is very loosely packed with a physical thickness of $\sim$100 μm by optical microscopy but with a negligible packing fraction of SWNTs. Thus we suggest that for measurement of intrinsic thermal and electrical properties of such loosely packed SWNT networks (Figure 1d), the optical density produces a more reliable metric of the effective film thickness than a measurement of the apparent physical thickness. Of course the optical density is directly related to the mass of SWNT material per unit area of the film.[10] The accuracy of measurement of the sample dimensions (10−20% in this study) is one of the principal factors determining the errors in the absolute value of the thermal conductivity of nanoscale size samples.[23]

For the thermal conductivity measurements, we utilized the bolometric configuration schematically presented in Figure 1a in which a narrow ribbon of semitransparent SWNT film is suspended across the opening in a sapphire ring (Figure 1b,c).[9] The electrical contacts to the SWNT sample were made with silver paste which is an efficient heat sink.[29] The length between electrical contacts (L) was 3.5−4.0 mm. The sapphire ring with SWNT film was mounted on the cold finger of a continuous flow helium optical cryostat with the sample space maintained at a pressure of <0.1 mTorr. The base temperature of the sapphire ring T_0 was measured using a Si diode temperature sensor, and a quartz filter at the base temperature T_0 was placed in the optical pathway above the SWNT film to limit the influence of blackbody radiation.

The heat was supplied by the radiation of an IR light emitting diode (LED, $\lambda_{MAX} = 940$ nm). The photoresponse of a suspended SWNT film is bolometric[9] and the absorbed IR radiation is efficiently converted to heat due to strong electron−phonon interaction; apparently the direct photoconductivity signal due to the generation of electrons (holes) in the conduction (valence) band is at least 5 orders of magnitude below the bolometric component.[9] We placed a 0.4 mm slit diaphragm in front of the sample (Figure 1a), so the IR LED uniformly illuminates a narrow central strip across the width of the SWNT film; in this geometry the thickness of the film t is much smaller than the film length L so the heat conduction can be treated as a one-dimensional problem. The absorbed heat Q propagates from the illuminated central region along the suspended SWNT film toward the electrical contacts without loss ($Q(x) = dT/dx = \text{const}$), thereby generating a triangular temperature profile with maximum temperature T_M in the middle (Figure 1a) and average temperature increment given by $\Delta T = (T_M -$

T_0)/2. In this geometry, the thermal conductivity κ of the SWNT film is determined by eq 1

$$\kappa = (P_{abs}/\Delta T)(L/8A) \quad (1)$$

where P_{abs} is the absorbed power of IR radiation and A is the cross-sectional area of the SWNT film. The factor of 8 in the denominator of eq 1 is a result of three factors of 2 that arise from the sample geometry: (i) half of the absorbed power flows to each of the contacts; (ii) the distance for the heat flow to reach a contact (heat sink) is $L/2$; and (iii) the average temperature increase, ΔT, is half the maximum temperature increase: $\Delta T = (T_M - T_0)/2$. The heat flow and temperature profile along the SWNT film are discussed in more detail in the Supporting Information together with an error analysis. It should be pointed out that because of the experimental geometry, eq 1 defines the in-plane thermal conductivity of SWNT film; it has been shown that under certain preparation conditions SWNT samples can be anisotropic[22,30] and the out-of-plane thermal conductivity can be below that measured in the plane.

The incident power P_{inc} was controlled by a function generator (in the range 0.1−20 μW), calibrated with a Perkin-Elmer VTB 6061 Si photodiode with radiometric sensitivity 0.50 A/W (940 nm) placed in the sample position. The absorbed power P_{abs} was obtained after correction of the incident power P_{inc} for the transmittance ($\mathscr{T}$) and diffuse reflectance ($\mathscr{R}$), according to $P_{abs} = P_{inc}(1 - \mathscr{T} - \mathscr{R})$; measurements were performed with a Cary 5000 UV−vis−NIR spectrophotometer. The diffuse reflectance at 940 nm was found to be at the level of 10% for nontransparent SWNT films (thickness, t > 500 nm) in accord with published data[31] and is further reduced in transparent thin films. The optical constants for semitransparent SWNT films were reported to be practically independent of temperature in the near-IR spectral range,[32] so we used the room-temperature values of $\mathscr{T}$ and $\mathscr{R}$ over the full temperature range.

The electrical resistance of the thin SWNT films utilized in these experiments is strongly temperature dependent[9,11] and can be used to measure the temperature modulation of the film. Figure 2a shows the electrical resistance of a SWNT film as it is cooled at a rate of 0.5 K/min under illumination by square-wave pulses of IR radiation at a frequency of 0.04 Hz; the power of the IR LED was adjusted from 20 to 0.2 μW in order to limit the temperature modulation to values of ΔT < 2K (T > 100 K) and ΔT < 0.5 K at low temperatures.

The ΔT data can be extracted directly from the amplitude of resistance modulation ΔR and the temperature dependence of the dark resistance dR/dT: $\Delta T = \Delta R/(\mathrm{d}R/\mathrm{d}T)$, as shown schematically in the Figure 2a.

The typical time constant for the thermal response is 50 ms, and with an 0.04 Hz frequency of modulation, an equilibrium temperature profile corresponding to eq 1 is established. Thus the present bolometric technique can be classified as an optical heating and electrical sensing method; other optical heating techniques such as the laser-flash

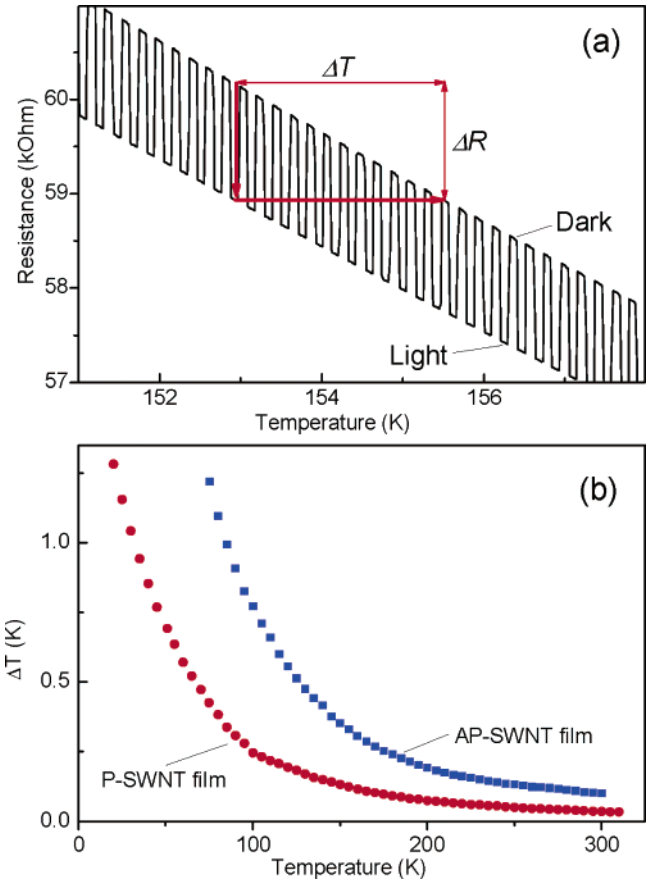

Figure 2. Bolometric determination of the thermal conductivity of AP- and P-SWNT films as a function of temperature by measurement of the SWNT film resistance under a 0.04 Hz square-wave illumination by an IR LED at a temperature sweep rate of 0.5 K/min. (a) The amplitude of the temperature increment ΔT of the SWNT film is determined from the amplitude of resistance modulation ΔR and the slope of temperature dependence of the dark resistance. (b) The amplitude of the temperature modulation of the SWNT films ΔT (normalized to an IR incident power of 1.0 μW).

diffusivity method require large samples, are in majority transient state pulsed methods, and thus require a knowledge of the heat capacity of the material in order to obtain the absolute value of κ.[23] The use of IR radiation as a heat source in the present technique, is alternative to the use of Joule heating in the 3ω technique[17−19,33] and removes the question of diffusive transport in the case of SWNTs where ballistic transport with no Joule heating may be significant.

Figure 2b presents temperature dependence $\Delta T(T)$ of an AP-SWNT film (t = 35 nm) and a P-SWNT film (t = 100 nm), at a normalized incident power, P_{inc} =1 μW.

The $\kappa(T)$ values were calculated from eq 1 on the basis of $\Delta T(T)$ data (Figure 2) and are presented in Figure 3a and were corrected for radiation heat losses $Q_{rad} \sim \Delta T^* T^3$,[23,29] where ΔT is the average difference between the temperature of suspended SWNT film and the temperature of the cold radiation shield surrounding the sample (Figure 1a). Figure 3a shows that radiation losses are significant for P-SWNT film at T > 150 K and for AP-SWNT films even at low temperatures. The accuracy of the correction was tested by measuring the thermal conductivity of a thick (t = 1 μm)

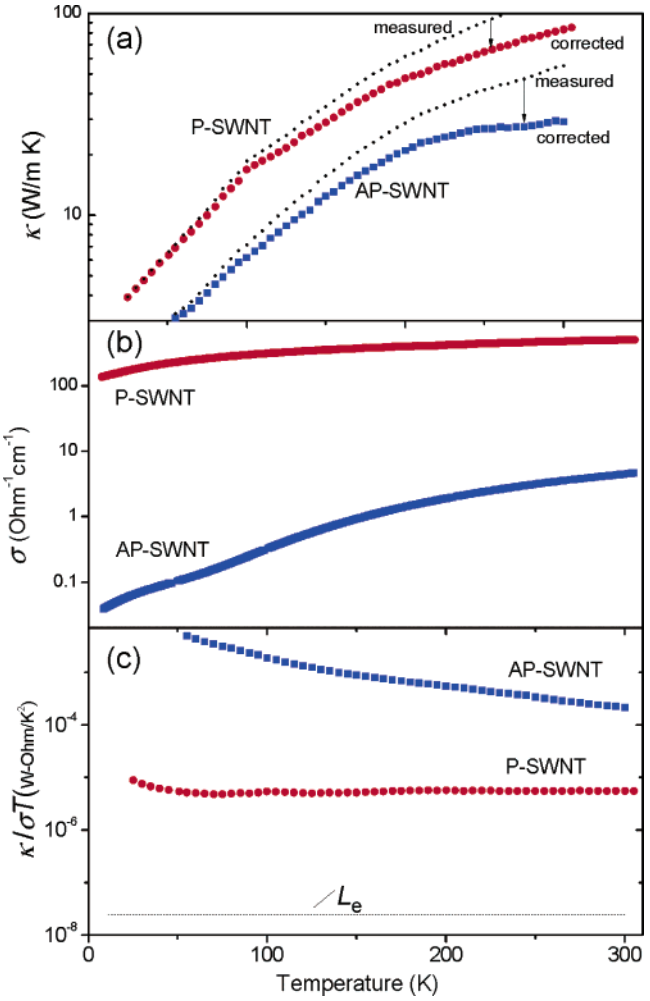

Figure 3. The temperature dependence of the transport properties of P-SWNT film of thickness 100 nm and AP-SWNT film of thickness 35 nm: (a) measured and corrected thermal conductivities; (b) electrical conductivities; (c) Lorenz numbers of the SWNT networks in comparison with the Lorenz number for a pure metal (L_e).

P-SWNT film (where radiation losses are insignificant), for which we obtained κ(300 K) $\approx$ 75 W/mK in satisfactory agreement with the corrected value for the thin film, κ(300 K) $\approx$ 83 W/mK (Figure 3a) and in the range of previously published data for SWNT buckypaper.[12,21,22] The radiation losses are intrinsic to the geometry of ultrathin films with large surface area to volume ratios.

For both the P-SWNT and AP-SWNT films, we observed a monotonic increase of thermal conductivity with increasing temperature and the $\kappa(T)$ behavior and absolute values of κ correlate with data obtained by the comparative technique.[12,20,22,30] The monotonic increase of κ with temperature has also been observed on individual SWNTs.[13,16] The absolute value of the thermal conductivity of the AP-SWNT film is κ(300 K) $\sim$ 30 W/mK (Figure 3a), which is about a factor of 3 below the value obtained for the P-SWNT film. These values are about 2 orders of magnitude below the intrinsic conductivity of individual SWNTs due to the thermal resistance of intertube junctions in the SWNT networks which are responsible for 97−99% of the total thermal resistance. In the case of the AP-SWNT films, intertube network junctions provide a weaker contact than those that exist in the P-SWNT network which is compacted during the vacuum filtration process; the SWNT intertube resistance may be affected by the degree of physical separation between the graphitic walls and the contact area at the junctions.[34,35]

The electrical conductivities (σ) of the same films are given in Figure 3b, and it is apparent that the differentiation is much more dramatic than in the case of thermal conductivity: for P-SWNT film σ(300 K) is about 2 orders of magnitude higher than that for the AP-SWNT film and this difference increases by a further 2 orders of magnitude at low temperatures. Both types of SWNT films show nonmetallic behavior suggesting the presence of tunneling barriers at the intertube junctions,[7,10−12] with much stronger suppression of electron tunneling in the case of AP-SWNTs. Thus the electron transport is more sensitive to the intertube junction than the phonon transport in these films.

The relative contribution of the electron and phonon components of the thermal conductivity can be evaluated on the basis of the Lorenz number, $L = \kappa/\sigma T$. As a point of reference, the Lorenz number for individual SWNTs may be obtained from experimental data in the literature for metallic SWNTs of diameter $\approx$2 nm and length $\approx$2.5 μm;[16] the reported thermal conductance $G \approx 2.4$ nW/K and electrical resistance $\rho \approx 5-6$ kΩ/μm[16] correspond to $\kappa \approx$ 3500 W/mK and $\sigma \approx 1.2 \times 10^6\ \Omega^{-1}\ \mathrm{cm}^{-1}$ thus giving $\kappa/\sigma T \approx 1 \times 10^{-7}$ W Ω/K^2 in comparison with the value of $L_e = 2.4453 \times 10^{-8}$ W Ω/K^2 for a pure metal where the thermal transport is predominantly electronic. Thus in individual metallic SWNTs the ratio of the electron and phonon contributions to the thermal conductivity is about 1:3.

The Lorenz number for the P-SWNT film, $\kappa/\sigma T$, is close to 7×10^{-6} W Ω/K^2 at temperatures between 50 and 300 K (Figure 3c), which corresponds to a ratio of the electron to phonon contribution to the thermal conductivity of 1 to 100, which is further decreased to 1 to 10 000 in the case of the AP-SWNT network ($\kappa/\sigma T \approx 4 \times 10^{-4}$ W Ω/K^2 at 300 K). Thus in a network both electron and phonon transport are suppressed by the intertube junction resistance, although the electron transport is more strongly suppressed resulting in an increase in the Lorentz number by 2−4 orders of magnitude (Figure 3). It is important to note that two out of three SWNTs in the network are semiconducting and do not contribute to the electron transport, while supporting the phonon flow.

We can compare the experimental Lorenz numbers for SWNT networks (Figure 3c) with published theoretical and experimental data on electrical and thermal transport on cross-junctions of individual nanotubes.[34−36] The electrical resistance at the junction of two metallic SWNTs was found to be 200 kΩ, contact of two semiconducting SWNTs showed a junction resistance of 500 kΩ, while contact of metallic and semiconducting SWNTs provided the most resistive junction (>10 MΩ) due to the Shottky barrier.[36] The heat conductance at intertube junctions G_J was evaluated theoretically not to exceed 10^{-9} W/K.[34,35] Assuming an average junction electrical resistance $R_J = 10^6\ \Omega$ we obtain

a Lorenz number for individual cross-junctions at 300 K of $L_J = R_J{*}G_J/T = 3 \times 10^{-6}$ W Ω/K^2 close to the value obtained for P-SWNT film and 2 orders of magnitude higher than the pure electronic value $L_e = 2.4453 \times 10^{-8}$ W Ω/K^2. This supports the conclusion that the heat transport across the intertube junction is dominated by the phonon component and also provides additional evidence for the idea that both the electrical and thermal transport in SWNT networks are dominated by intertube junctions.

Stronger suppression of electrical conductivity and larger Lorenz numbers ($\sim 10^{-2}$ W Ω/K^2) were observed in case of a SWNT network embedded in a polymer matrix.[8] In this case the presence of a very thin ($\sim$1 nm) layer of polymer separating the SWNTs probably dominates the intertube junction resistance.[8,34,35] This interfacial layer acts as an insulating barrier which introduces phonon scattering and significantly suppresses electron tunneling. The wide variations in the Lorenz numbers may be attributed to high sensitivity of the electron transport to the specifics of the intertube junctions (Figure 3c), in part because the electrical conductivities of materials span many orders of magnitude whereas thermal conductivities are much less material specific.[8,35] The electrical conductivity of SWNT networks is strongly modified by chemical functionalization;[11] controlling the thermal conductivity appears to be a much more difficult task, although the introduction of SWNT side-wall functional groups may allow some degree of tuning of the thermal conductivity.[37]

In summary, we introduced a bolometric technique for the measurement of the thermal conductivity of ultrathin SWNT films, which is ideally suited for nanoscale size SWNT films with strong IR absorption and temperature-dependent resistance and is particularly useful for optimization of the sensitive element of the SWNT-based IR detector.[9] The thermal and electrical transport properties of the SWNT networks are extremely sensitive to morphology, dispersion, and the nature of the intertube junctions which can be utilized for optimization of SWNT networks for specific applications.

Acknowledgment. This research was supported by DOD/DMEA under Awards No. H94003-06-2-0608 and No. H94003-06-20604. F.B. acknowledges support from a Fulbright Association.

Supporting Information Available: Description of temperature distribution along suspended SWNT film and comparison of the thermal and electrical transport in SWNT films and SWNT/epoxy composites. This material is available free of charge via the Internet at http://pubs.acs.org.

References

(1) Bekyarova, E.; Davis, M.; Burch, T.; Itkis, M. E.; Zhao, B.; Sunshine, S.; Haddon, R. C. *J. Phys. Chem. B* **2004**, *108*, 19717−19720.
(2) Snow, E. S.; Perkins, F. K.; Houser, E. J.; Badescu, S. C.; Reinecke, T. L. *Science* **2005**, *307*, 1942−1945.
(3) Wu, Z.; Chen, Z.; Du, X.; Logan, J. M.; Sippel, J.; Nikolou, M.; Kamaras, K.; Reynolds, J. R.; Tanner, D. B.; Hebard, A. F.; Rinzler, A. G. *Science* **2004**, *305*, 1273−1276.
(4) Artukovic, E.; Kaempgen, M.; Hetch, D. S.; Roth, S.; Gruner, G. *Nano Lett.* **2005**, *5*, 757−760.
(5) Zhang, M.; Fang, S.; Zakhidov, A. A.; Lee, S. B.; Aliev, A. E.; Williams, C.; Atkinson, K. R.; Baughman, R. H. *Science* **2005**, *309*, 1215−1219.
(6) Zhang, D.; Ryu, K.; Liu, X.; Polikarpov, E.; Ly, J.; Tompson, M. E.; Zhou, C. *Nano Lett.* **2006**, *6*, 1880−1886.
(7) Gruner, G. *J. Mater. Chem.* **2006**, *16*, 3533−3539.
(8) Yu, A.; Itkis, M. E.; Bekyarova, E.; Haddon, R. C. *Appl. Phys. Lett.* **2006**, *89*, 133102.
(9) Itkis, M. E.; Borondics, F.; Yu, A.; Haddon, R. C. *Science* **2006**, *312*, 413−416.
(10) Hu, L.; Hecht, D. S.; Gruner, G. *Nano Lett.* **2004**, *4*, 2513−2517.
(11) Bekyarova, E.; Itkis, M. E.; Cabrera, N.; Zhao, B.; Yu, A.; Gao, J.; Haddon, R. C. *J. Am. Chem. Soc.* **2005**, *127*, 5990−5995.
(12) Hone, J.; Llaguno, M. C.; Nemes, N. M.; Johnson, A. T.; Fischer, J. E.; Walters, D. A.; Casavant, M. J.; Schmidt, J.; Smalley, R. E. *Appl. Phys. Lett.* **2000**, *77*, 666−668.
(13) Yu, C. H.; Shi, L.; Yao, Z.; Li, D. Y.; Majumdar, A. *Nano Lett.* **2005**, *5*, 1842−1846.
(14) Kim, P.; Shi, L.; Majumdar, A.; McEuen, P. L. *Phys. Rev. Lett.* **2001**, *87*, 215502.
(15) Fujii, M.; Zhang, X.; Xie, H. Q.; Ago, H.; Takahashi, K.; Ikuta, T.; Abe, H.; Shimizu, T. *Phys. Rev. Lett.* **2005**, *95*, 065502.
(16) Pop, E.; Mann, D.; Wang, Q.; Goodson, K.; Dai, H. J. *Nano Lett.* **2006**, *6*, 96−100.
(17) Yi, W.; Lu, L.; Dian-lin, Z.; Pan, Z. W.; Xie, S. S. *Phys. Rev. B* **1999**, *59*, R9015−R9018.
(18) Choi, T. Y.; Poulikakos, D.; Tharian, J.; Sennhauser, U. *Appl. Phys. Lett.* **2005**, *87*, 013108.
(19) Choi, T. Y.; Poulikakos, D.; Tharian, J.; Sennhauser, U. *Nano Lett.* **2006**, *6*, 1589−1593.
(20) Hone, J.; Whitney, M.; Piskoti, C.; Zettl, A. *Phys. Rev. B* **1999**, *59*, R2514−R2516.
(21) Hone, J.; Liaguno, M. C.; Biercuk, M. J.; Johnson, A. T.; Batlogg, B.; Benes, Z.; Fischer, J. E. *Appl. Phys. A* **2002**, *74*, 339−343.
(22) Gonnet, P.; Liang, Z.; Choi, E. S.; Kadambala, R. S.; Zhang, C.; Brooks, J. S.; Wang, B.; Kramer, L. *Curr. Appl. Phys.* **2006**, *6*, 119−122.
(23) Tritt, T. M. *Thermal Conductivity: Theory, Properties and Applications*; Kluwer Academic/Plenum Publishers: New York, 2004.
(24) Itkis, M. E.; Perea, D.; Niyogi, S.; Love, J.; Tang, J.; Yu, A.; Kang, C.; Jung, R.; Haddon, R. C. *J. Phys. Chem. B* **2004**, *108*, 12770−12775.
(25) Yu, A.; Bekyarova, E.; Itkis, M. E.; Fakhrutdinov, D.; Webster, R.; Haddon, R. C. *J. Am. Chem. Soc.* **2006**, *128*, 9902−9908.
(26) Gao, G.; Cagin, T.; Goddard, W. A., III *Nanotechnology* **1998**, *9*, 184−191.
(27) Zhao, B.; Itkis, M. E.; Niyogi, S.; Hu, H.; Perea, D.; Haddon, R. C. *J. Nanosci. Nanotechnol.* **2004**, *4*, 995−1004.
(28) Zhao, B.; Itkis, M. E.; Niyogi, S.; Hu, H.; Zhang, J.; Haddon, R. C. *J. Phys. Chem. B* **2004**, *108*, 8136−8141.
(29) Zawilski, B. M.; Littleton, R. T.; Tritt, T. M. *Rev. Sci. Instrum.* **2001**, *72*, 1770−1774.
(30) Fischer, J. E.; Zhou, W.; Vavro, J.; Liaguno, M. C.; Guthy, G.; Haggenmueller, R.; Casavant, M. J.; Walters, D. E.; Smalley, R. E. *J. Appl. Phys.* **2003**, *93*, 2157−2163.
(31) Zhou, W.; Vavro, J.; Nemes, N. M.; Fischer, J. E.; Borondics, F.; Kamaras, K.; Tanner, D. B. *Phys. Rev. B* **2005**, *71*, 205423.
(32) Borondics, F.; Kamaras, K.; Nikolou, M.; Tanner, D. B.; Chen, Z. H.; Rinzler, A. G. *Phys Rev. B* **2006**, *74*, 045431.
(33) Borca-Tasciuc, D. A.; Pietruzska, L.; Borca-Tasciuc, T.; Vajtai, R.; Ajayan, P. M., 21st IEEE Semiconductor Thermal Measurement and Management (SEMI-THERM) Symposium, San Jose, CA, 2005, p 283.
(34) Shenogin, S.; Xue, L. P.; Ozisik, R.; Keblinski, P.; Cahill, D. G. *J. Appl. Phys.* **2004**, *95*, 8136−8144.
(35) Shenogina, N.; Shenogin, S.; Xue, L.; Keblinski, P. *Appl. Phys. Lett.* **2005**, *87*, 133106.
(36) Fuhrer, M. S.; Nygard, J.; Shih, L.; Forero, M.; Yoon, Y.-G.; Mazzoni, M. S. C.; Choi, H. J.; Ihm, J.; Louie, S. G.; Zettl, A.; McEuen, P. L. *Science* **2000**, *288*, 494−497.
(37) Shenogin, S.; Bodapati, A.; Xue, L.; Ozisik, R.; Keblinski, P. *Appl. Phys. Lett.* **2004**, *85*, 2229−2231.

NL062689X